NASA TECHNICAL NOTE

NASA TN D-5997

NASA TN D-5997

MECHANICAL PROPERTIES OF ADVANCED GRAVITY GRADIENT BOOMS

by C. L. Staugaitis and R. E. Predmore

Goddard Space Flight Center
Greenbelt, Md. 20771

NATIONAL AERONAUTICS AND SPACE ADMINISTRATION • WASHINGTON, D. C. • OCTOBER 1970

1. Report No. NASA TN D-5997
2. Government Accession No.
3. Recipient's Catalog No.

4. Title and Subtitle

Mechanical Properties of Advanced Gravity Gradient Booms

5. Report Date October 1970
6. Performing Organization Code

7. Author(s) C. L. Staugaitis and R. E. Predmore

8. Performing Organization Report No. G-999
9. Performing Organization Name and Address

Goddard Space Flight Center
Greenbelt, Maryland 20771

10. Work Unit No.
11. Contract or Grant No.
13. Type of Report and Period Covered

Technical Note

12. Sponsoring Agency Name and Address

National Aeronautics and Space Administration
Washington, D.C. 20546

14. Sponsoring Agency Code
15. Supplementary Notes

16. Abstract

The mechanical (static and dynamic) behavior of a number of boom designs applicable to gravity gradient and antenna use were investigated.

Bending stiffness, critical bending moment, damping, and transverse (fundamental bending) frequency were the principal properties measured. The structural integrity of two boom designs was also evaluated when subjected to cyclic loading conditions.

The results are analyzed in terms of structural performance and conformance to elastic behavior as predicted by theory for thin-walled tubes.

17. Key Words Suggested by Author

Gravity gradient booms
Damping
Bending stiffness
Buckling

18. Distribution Statement

Unclassified-Unlimited

19. Security Classif. (of this report)	20. Security Classif. (of this page)	21. No. of Pages	22. Price*
Unclassified	Unclassified	29	$3.00

*For sale by the Clearinghouse for Federal Scientific and Technical Information
Springfield, Virginia 22151

CONTENTS

MECHANICAL PROPERTIES OF ADVANCED GRAVITY GRADIENT BOOMS

by

C. L. Staugaitis and R. E. Predmore
Goddard Space Flight Center

INTRODUCTION

Thin-walled tubular structures of open cross section have been used on a variety of spacecraft (e.g., OGO, RAE, and DODGE) as antennae and remote sensing probes, and for passive (gravity gradient) stabilization. These booms are inevitably subjected to a variety of mechanical and thermal loads during qualification, launch, and spaceflight operations. In addition, such environmental factors as radiation, micrometeoroid impingement, and vacuum can pose serious problems for long-term service reliability.

Initially, a preponderant number of such boom elements consisted of the DeHavilland* STEM, henceforth referred to as SPAR-STEM, simply because it represented the only configuration readily available. Essentially, the SPAR-STEM (Reference 1) (STEM is an acronym for storable tubular extendible member) is an overlapped boom of circular cross section with a bending stiffness comparable to a dimensionally similar seamless tube. Although the structural adequacy of the SPAR-STEM had been demonstrated for relatively short lengths, the performance of this particular geometric configuration became questionable in anticipation of much greater length requirements, on the order of 1000 ft. Specifically, the SPAR-STEM's overlapped seam offers negligible torsional rigidity when combined with significant thermal bending, which seriously degrades its usefulness, especially in the case of passive stabilization, for which booms provide the primary means for maintaining spacecraft attitude control. As a consequence of this apparent design deficiency, GSFC (Reference 2) inaugurated an extensive boom-materials program to develop advanced boom designs together with compatible deployment mechanisms.

This report presents the mechanical characteristics of these boom configurations and, where possible, relates them to SPAR-STEM behavior. Bending stiffness, critical bending moment, damping, and fundamental bending frequency were measured, and in addition, the results of cyclic loading on two of the booms investigated are reported.

*On January 1, 1968, SPAR Division of DeHavilland Aircraft of Canada Limited became incorporated under the name of SPAR Aerospace Products, Ltd., Malton, Ontario.

An in-house investigation concerned with boom thermal static bending plus twist behavior is currently in progress and will form the subject of a future report.

CONFIGURATION OF GRAVITY GRADIENT BOOMS

The boom designs described in this report are shown in Figure 1 and reflect developments by the General Electric Co., Valley Forge, Pa.; the General Dynamics Corp./ Convair Division, San Diego, Calif., and the Westinghouse Electric Corp., Baltimore, Md. The boom designs investigated exhibit a "memory" when extended; i.e., they form a tubular shape from an originally flattened strip when they are relieved of all restraint.

BeCu ALLOY,OVERLAPPED,DeHAVILLAND STEM

MOLYBDENUM,OVERLAPPED,GENERAL ELECTRIC BOOM

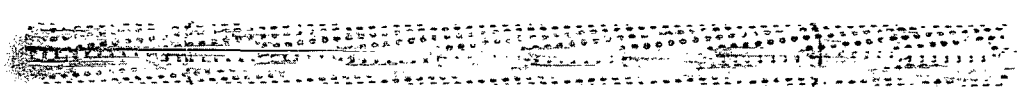

PERFORATED,INTERLOCKED,WESTINGHOUSE BOOM

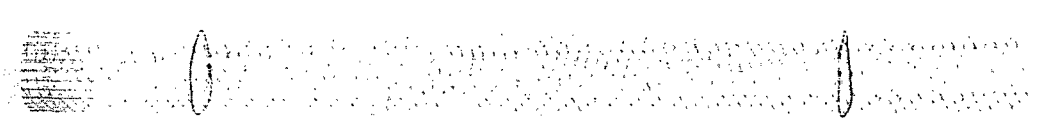

WIRE GRID,OVERLAPPED,GENERAL DYNAMICS/CONVAIR BOOM

Figure 1–Gravity gradient booms.

Overlapped BeCu SPAR-STEM

The SPAR-STEM configuration represents (nominally) a 0.5-in.-diameter tube that is made from a 0.002-in.-thick by 2.0-in.-wide partially aged BeCu alloy 25 strip. The strip passes through a series of forming dies designed to cold shape it gradually into a circular configuration followed by a heat treatment that stabilizes the strip as a permanently overlapped tube. The heat treatment stage of the forming operation is achieved by developing a proper balance of two complex mechanisms, aging and stress relief, which act simultaneously. The tube is then wound on a drum by means of guide rollers, which promotes the transition from the tubular to the flat condition (ploy shape).

Overlapped Molybdenum General Electric Boom

Basically, the General Electric overlapped molybdenum boom (Reference 3) is very similar to the previously described SPAR-STEM design, except that the strip material and forming practice used are different. The boom is fabricated from 0.001-in.-thick by 2-in.-wide unalloyed (99.99% pure powder metallurgy) molybdenum foil. This refractory metal was selected because of such desirable characteristics as high thermal conductivity, low thermal expansion coefficient, high elastic modulus, and high tensile strength. Another important factor in the selection of molybdenum was its ability to develop the required "memory" in the strip without requiring a precise precipitation heat treatment.

Essentially, the as-received strip is cold formed through an array of drawing dies into a circular configuration, at which point it enters the constraining tube within an electrical resistance heated furnace. The constrained shape is then subjected to a prescribed stress-relief heat treatment cycle sufficient to reduce the magnitude of both the induced rolling and the forming stresses and thus to set permanently the overlapped tubular shape.

Overlapped Dual-Wire Screen General Dynamics/ Convair Boom

The General Dynamics/Convair overlapped dual-wire screen boom (References 4 and 5) is a unique bimetallic tubular structure formed to a nominal diameter of 0.75 in. The longitudinal strand consists of 0.009-in.-diameter Elgiloy (cobalt base alloy), and a 0.007-in.-diameter BeCu alloy 25 wire is employed in the circumferential direction. The wire screen is optimized to a 16-wire/in. - by - 18-wire/in. mesh size corresponding to an open area of approximately 76%. The boom-forming schedule can be divided into three major steps:

(1) The raw screen (woven by conventional loom practice) is made rigid at the nodes by means of a vertical strip brazing furnace.

(2) The rigid screen is then stretched to impart cold work, necessary for optimum response to heat treatment and development of desired strength properties, to the Elgiloy wires.

(3) The screen is then fed into a funnel that transforms the flat strip to a circular shape before it enters a stainless steel tube within an argon-filled continuous furnace. The subsequent age-forming treatment fixes the overlapped tubular shape, which promotes the necessary elastic response.

The bimetallic approach was taken because thermal conductivity is very important in the circumferential directions but not as important in the longitudinal directions. However, thermal expansion is a critical parameter in the longitudinal direction but has very little radial effect. Therefore, because of its good thermal conductivity, BeCu was chosen for the circumferential wire, and Elgiloy was selected for the longitudinal direction, not only because its coefficient of thermal expansion is approximately 25% less, but also because its ultimate tensile strength is over 350 000 psi, a very desirable strength level.

Interlocked Perforated Westinghouse Boom

The Westinghouse interlocked perforated boom* is a 0.50-in.-diameter BeCu alloy 25 tubular element with approximately a 17% open area in a precisely holed helical pattern designed to "average out" solar irradiation absorbed on both the internal and external boom surfaces. Such a design provides an edge-zippering (positive locking) capability that markedly improves torsional rigidity several orders of magnitude over that of the SPAR-STEM design, a most desirable property from the dynamic viewpoint. The machining of perforations and edge notches is performed by chemical milling, an approach that leaves the strip material completely undisturbed in contrast to such operations as stamping, blanking, or punching.

The starting strip is 0.002 in. thick by 2 in. wide in the 1/2 H temper. The hole pattern is developed by applying an ultraviolet photo resist, exposing the photo resist through a master mask, and chemically etching the exposed areas, which reduces the width to 1.75 in. Then, the strip is fed into a tab bender that sets the tabs at the correct angle for insuring proper zippering action. A chemically converted black copper oxide coating (Ebonol C) is applied to the inside of the strip, and a highly reflective aluminum plate is vacuum deposited on the outside. Finally, the strip is pulled through a forming funnel into a precision glass tube within the furnace where it is heat treated to form the desired interlocked tubular shape.

STRUCTURAL PROPERTIES OF BOOM ELEMENTS

Bending Stiffness

An important structural characteristic is bending stiffness EI, which is the product of the elastic modulus E and the area moment of inertia I. Static and dynamic EI values

*"Gravity Gradient Stabilization System Elements and Antenna Structures," Westinghouse Defense and Space Center. NAS5-9598. December 1965.

were determined with a test setup consisting essentially of a clamped-free cantilevered elastic boom, as seen in Figures 2 and 3, respectively. The corresponding coordinate system describing boom motion is shown in Figure 4.

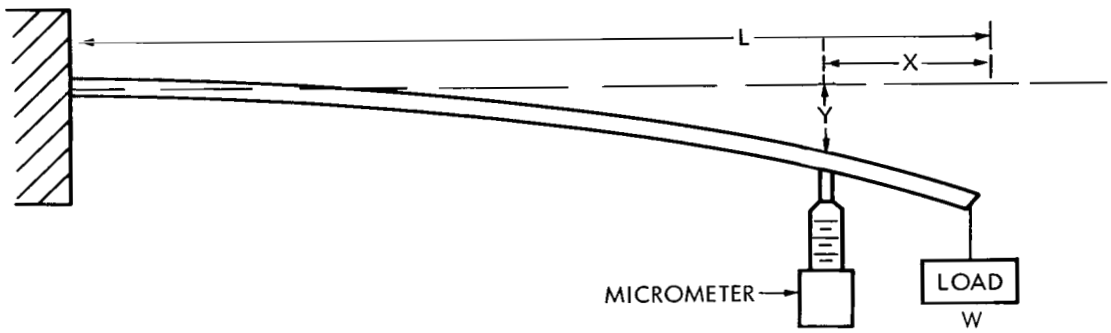

Figure 2–Static bend test setup.

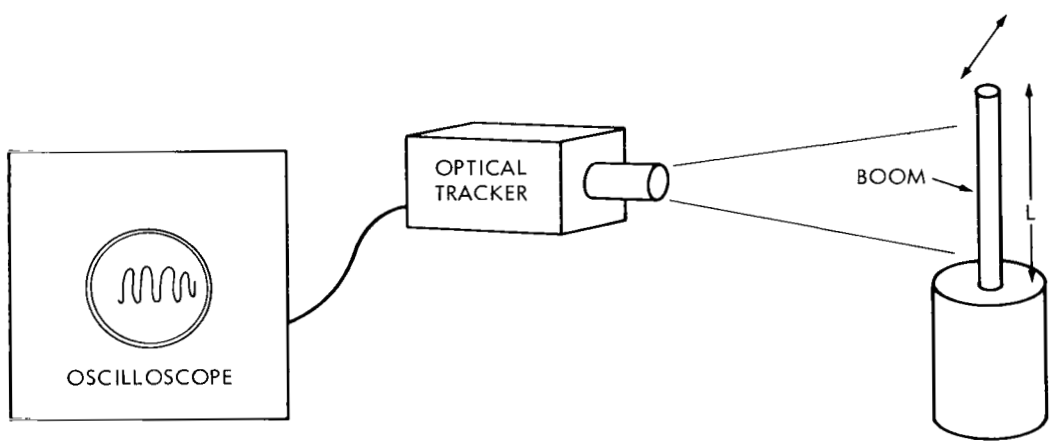

Figure 3–Apparatus used to measure the vibration frequency of a clamped-free cantilever boom.

The static EI was calculated from the tip load and tip deflection data and is graphically summarized in Figures 5 through 11. Equation 1 is the conventional elastic beam equation for static EI:

$$EI = \frac{W(X^3 - 3L^2X + 2L^3)}{6Y}, \qquad (1)$$

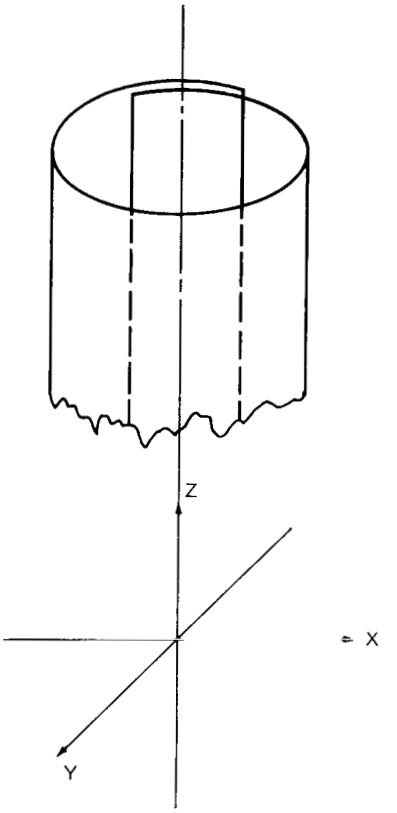

Figure 4–Coordinates describing the gravity gradient boom.

where

Y = tip deflection (in.)

EI = static bending stiffness (lb-in.^{2})

E = modulus of elasticity (lb/in.^{2})

I = moment of inertia (in.^{4})

W = load (lb)

L = length (load to root) (in.)

X = length (load position to position of deflection measurements) (in.).

Dynamic EI measurements were obtained for a vibrating boom segment clamped vertically at its base. The boom was displaced laterally and allowed to oscillate at its fundamental bending frequency. The decaying vibration was subsequently recorded normal to the plane of motion by means of an optical tracker in conjunction with an image storage oscilloscope. Dynamic EI was calculated according to Equation 2:

$$EI = \mu L^4 \left(\frac{w}{A}\right)^2, \tag{2}$$

where

EI = dynamic boom stiffness (lb-in.^{2})

E = modulus of elasticity (lb/in.^{2})

I = moment of inertia (in.^{4})

μ = mass per unit (lb-sec^2/in.^{2})

L = length (root to tip) (in.)

w = natural frequency (rad/sec)

A = constant for clamped-free cantilever beam of uniform mass distribution.

Except for the SPAR-STEM, these booms represent relatively recent developments. Pertinent dimensional and geometric descriptions of the booms tested are summarized in Table 1, while stiffness data are presented in Table 2.

Overlapped BeCu Alloy SPAR-STEM

The tip load versus tip deflection relations are graphically presented in Figure 5 from which static EI was calculated to be 1720 lb-in.^{2} and 2170 lb-in.^{2} in the EI_x and the EI_y orientations, respectively. These static EI's are comparable to previous results (also included in Table 2) conducted on similar booms.

Measured boom frequencies in the x- and y-planes are 11.4 Hz and 14.1 Hz, respectively. The corresponding dynamic EI values computed from equation 2 are 1790 lb-in.^{2} and 2740 lb-in.^{2}. The higher dynamic EI's evidenced, especially in the y-plane, are attributed to the development of higher root stressing and consequent nonlinear load-deflection behavior promoted by the clamped-free cantilevered booms peculiar to the static test method. These dynamic measurements of EI are in reasonable agreement with values derived theoretically (Reference 6) (EI_x = 2150 lb-in.^{2}, and

Table 1-Description of test booms for stiffness measurements.

Boom design	Material	Manufacturer	Tape width (in.)	Tape thickness (in.)	Diameter (in.)	Seam overlap (degrees)	Boom length (in.)		Weight length ($\times 10^{-3}$ lb/in.)
							static test	dynamic test	
Overlapped SPAR-STEM	BeCu	SPAR Products, Ltd.	2.0	0.002	0.47	100	32.0	34.1	1.236
Overlapped									
Straight seam	Molybdenum	General Electric	2.0	.0011	.50	100	34.7	35.0	.795
Twisted seam (45°/36 in.)	Molybdenum	General Electric	2.0	.0016	.50	100	34.7	35.0	.903
Overlapped wire grid									
12 x 17 mesh	BeCu Elgiloy	General Dynamics/Convair	2.4	*	.75	35	34.7	35.0	1.150
12 x 12 mesh	BeCu Elgiloy	General Dynamics/Convair	2.5	*	.75	75	34.7	35.0	1.055
Interlocked perforated									
0% perforations	BeCu	Westinghouse	1.75	.002	.50	30	32.0	34.5	1.059
15% perforations	BeCu	Westinghouse	1.75	.002	.50	30	32.0	34.5	.874
30% perforations	BeCu	Westinghouse	1.75	.002	.50	30	32.0	34.6	.692
45% perforations	BeCu	Westinghouse	1.75	.002	.50	30	32.0	34.7	.562
15% perforations, tight seam	BeCu	Westinghouse	1.75	.002	.50	30	34.5	35.0	.877
15% perforations, moderately tight seam	BeCu	Westinghouse	1.75	.002	.50	30	34.5	35.0	.877
15% perforations, loose seam	BeCu	Westinghouse	1.75	.002	.50	30	34.5	35.0	.863

*0.0083-in.-diameter Elgiloy wire (longitudinal), 0.0073-in.-diameter BeCu wire (transverse).

Table 2-Bending stiffness, EI (lb-in.^{2}).

Boom design		Dynamic		Static				Static		Average EI	
		EI_x	EI_y	EI_{+x}	EI_{-x}	EI_{+y}	EI_{-y}	EI_x(av)	EI_y(av)	Static	Dynamic
BeCu overlapped SPAR-STEM		1790	2740	1720		2170				1950	2270
				1730*	1520*	2300*	2180*	1620*	2240*	1930*	
Molybdenum overlapped											
Straight seam		1660	2520	1210	1990	2240	2030	1600	2140	1870	2090
Twisted seam		2170	2500	2200	2200	2570	2200	2200	2380	2290	2340
Wire grid overlapped											
12 x 17 mesh		1570	2220	1300	1080	2510	1700	1190	2110	1650	1900
12 x 12 mesh		1060	2390	900	976	2500	2030	940	2270	1600	1720
BeCu interlocked perforated											
Moderately tight seam											
0% perforations		1950	1850	1720		1640					
15% perforations		1260	1030	1110		930					
30% perforations		810	690	710		620					
45% perforations		550	460	460		410					
15% perforations, tight seam	Low	1230	1080	1010	1170	990	950	1090	970	1030	1160
15% perforations, moderately tight seam	bending	1190	1020	1060	1090	920	910	1080	920	1000	1110
15% perforations, loose seam	moment	1150	1000	1040	1020	890	870	1030	880	960	1080
15% perforations, tight seam	High	1020	880								950
15% perforations, moderately tight seam	bending	1080	840								960
15% perforations, loose seam	moment	1070	910								990

*Results of earlier tests on 3-ft-long booms, with a nominal diameter of 0.500 in. and an overlap of approximately 100°.

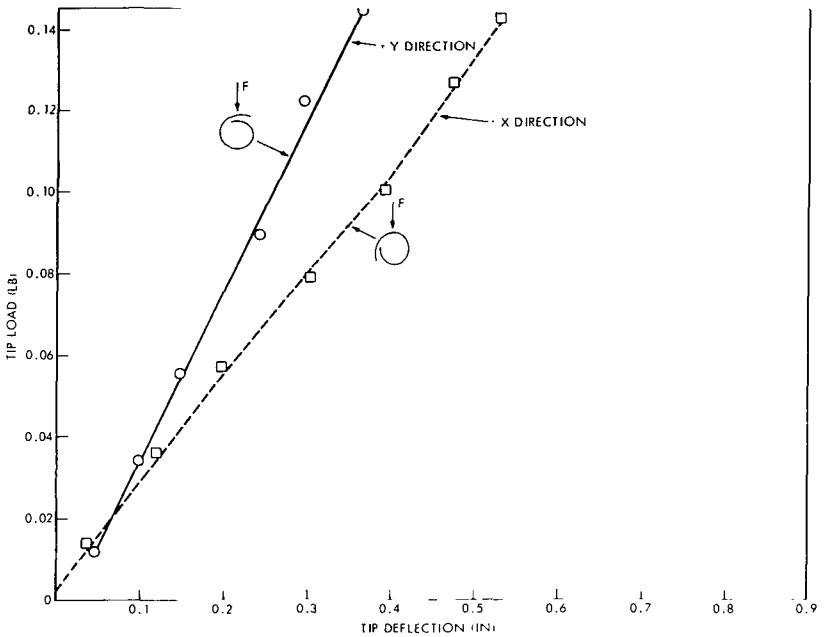

Figure 5–Load-deflection curve of a BeCu overlapped SPAR-STEM cantilever clamped-free boom. Seam overlap angle, 100°; length, 32 in.; surface condition, BeCu alloy.

EI_y = 2620 lb-in.^{2}) but are at least 20% greater than values obtained by static means. Regardless of the test method, the EI of thin-walled cylinders of open section is always significantly higher in the y-plane than in the x-plane of loading. This can be explained by the existence of the double-wall thickness due to the overlapped seam and consequent increase in I.

Overlapped Molybdenum General Electric Boom

As indicated in Table 1, the two molybdenum specimens* differed in two respects, a distinct variation in initial strip thickness and the degree of seam straightness. In the case of the latter, one of the tubular specimens incorporated a spiral in the seam of approximately 45° in a length of 36 in. The variation in strip thickness is reflected in the observed difference in weight per unit length of the tubular elements as indicated in Table 1. Both static EI specimens were 34.7 in. long, with the tip deflection recorded 3.3 in. below the point at which the load is applied. The tip load versus tip deflection relation is shown in Figure 6 for the boom with a straight seam. The experimental EI's for the molybdenum tube with straight seam are EI_x = 1210 lb-in.^{2} and EI_y = 2240 lb-in.^{2}. These data are lower than the corresponding, but more uniform, dynamic EI values of EI_x = 2170 lb-in.^{2} and EI_y = 2500 lb-in.^{2} calculated from the data in Figure 7. This

*Mink, Fred V., "Static and Dynamic Mechanical Properties of Gravity Gradient Booms," Melpar, Inc. NAS5-3753. January 1967.

stiffness behavior of the special molybdenum element is explained by the "averaging" effect of the helical seam on section properties in contrast to the geometric bias (e.g., in I) inevitable with the straight seam configurations.

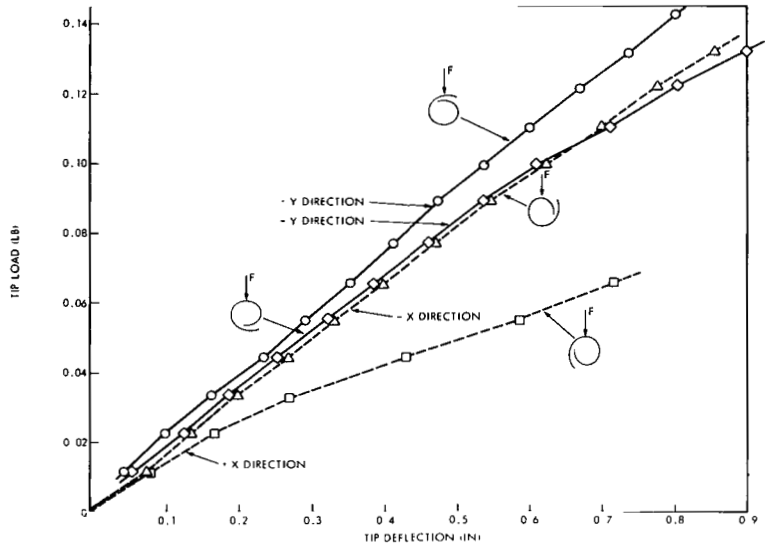

Figure 6—Load-deflection curve of a molybdenum overlapped General Electric cantilever clamped-free boom. Length, 34.7 in.; thickness, 0.0011 in.; twist of seams, 0°/36 in. of length.

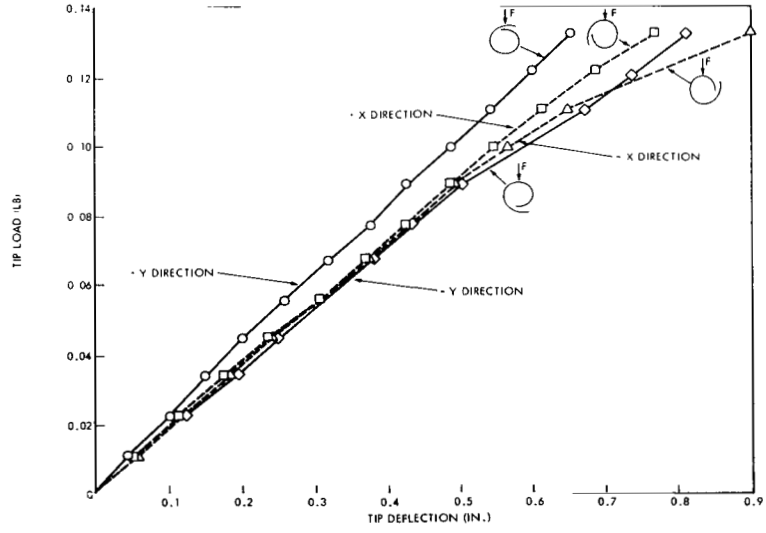

Figure 7—Load-deflection curve of a molybdenum overlapped General Electric twisted seam cantilever clamped-free boom. Length, 34.7 in.; thickness, 0.0016 in.; twist of seam, 45°/36 in. of length.

Overlapped Wire Grid General Dynamics/Convair Boom

The two wire grid elements investigated represented not only different mesh sizes but differences in degree of overlap as well. The statically loaded horizontal tubes were 34.8 in. long, while the clamped-free vibrating tubes were 35 in. long. The static tip deflection measurements are shown in Figures 8 and 9. The EI values in the y-plane

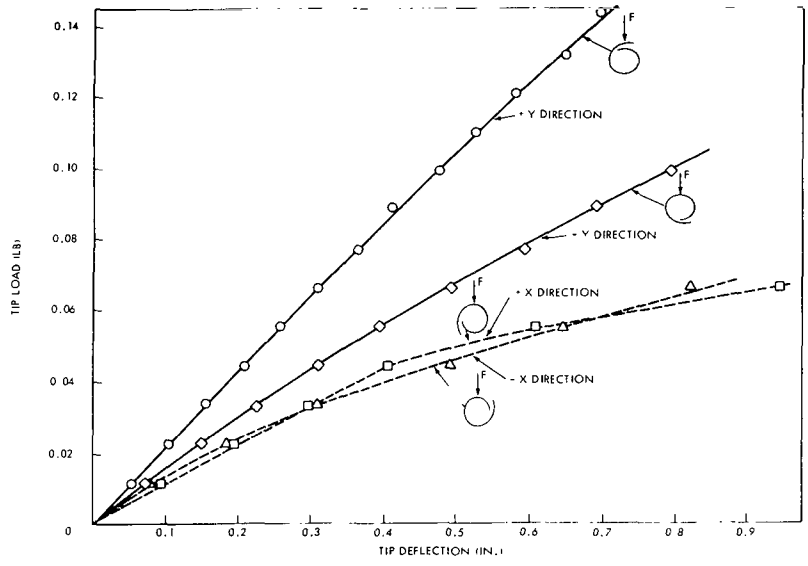

Figure 8–Load-deflection curve of a wire grid overlapped General Dynamics/Convair 12 by 17 cantilever clamped-free boom. Longitudinal wires, 12 wires per in.; cross wires, 17 wires per in.; length, 34.7 in.; seam overlap angle, 35°; twist of seam, 0°/36 in. of length.

obtained for the 12 by 17 and 12 by 12 mesh sizes were the same ($EI_y = 2510$ lb-in.^{2}), but in the x-plane, they were 1300 lb-in.^{2} and 900 lb-in.^{2}, respectively. Consistent with the overlapped configuration, the dynamic EI's were again significantly higher than the corresponding static EI's by 13% for the 12 by 12 mesh size and 7% for the 12 by 17 mesh size.

Interlocked Perforated Westinghouse Boom

Stiffness determinations were obtained on seven boom segments incorporating 0%, 15%, 30%, and 45% perforations, the dimensions of which are described in Table 1. In addition, some of the booms were deliberately processed to encompass a range of seam tightness (defined by the degree of interlocking force developed between mating tabs) arbitrarily designated as tight, moderately tight, and loose. The seam interlocking force is proportional to the unzippered diameter of the unlocked boom. The unzippered diameters of the tight, moderately tight, and relatively loose interlocked seams were 0.365 in., 0.383 in., and 0.409 in., respectively. The asymmetric nature of the booms' cross sections is evident from comparison of zippered diameters in both the x- and y-planes.

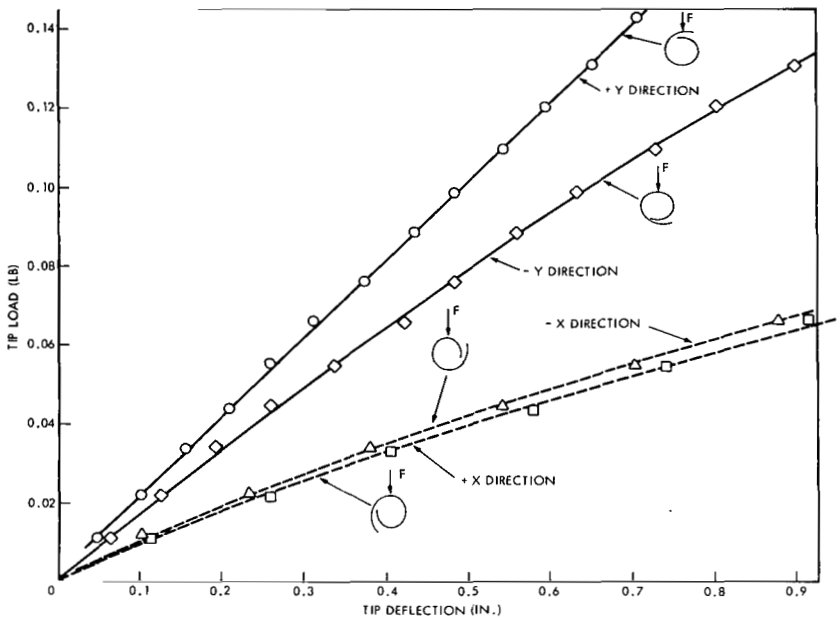

Figure 9—Load-deflection curve of a wire grid overlapped General Dynamics/Convair 12 by 12 cantilever clamped-free boom. Longitudinal wires, 12 wires per in.; cross wires, 12 wires per in.; length, 34.7 in.; seam overlap angle, 75°; twist of seam, 0°/36 in. of length.

For example, the diameter of the tight and moderately tight booms was 0.515 in. in the x-plane and 0.470 in. in the y-plane, while the diameter of the loose boom measured 0.515 in. in the x-plane and 0.495 in. in the y-plane.

The results of tip load versus tip deflection for the four ranges of perforations are shown in Figure 10, and the influence of seam orientation and interlocking force on bend behavior is indicated by the results of Figure 11 for the 15% perforated element. The pronounced effect of hole area on EI magnitude is clearly evident in Table 2. Perforating 45% of the boom area reduces the average EI in the x-plane from 1950 lb-in.^{2} to 550 lb-in.^{2} (~ 72%). A similar reduction in stiffness from 1850 lb-in.^{2} to 460 lb-in.^{2} is noted in the y-plane. Consistent with the trend for the other three types of booms, the dynamic EI constants were greater than the corresponding static EI constants. However, the x-plane EI was observed to be 10% to 20% greater than that for the y-plane, which is contrary to the EI behavior exhibited by the other three overlapped boom configurations. This is attributed to the cross-sectional variations present in both the open (overlapped) and closed (interlocked) configurations and their respective effects on EI properties. For an open thin-walled cylinder, EI is proportional to wall thickness and the cube of the radius. Obviously, a relatively small change in radius will alter EI characteristics more than a similar change in wall thickness. Geometrically, the overlapped structures are essentially circular in cross section in contrast to the elliptical profile assumed by the zippered boom. It is not surprising, therefore, to find that the value for I, and consequently for EI, in the plane of the seam (y-plane) for the overlapped boom is larger than in the x-plane simply because the wall thickness has been doubled. The

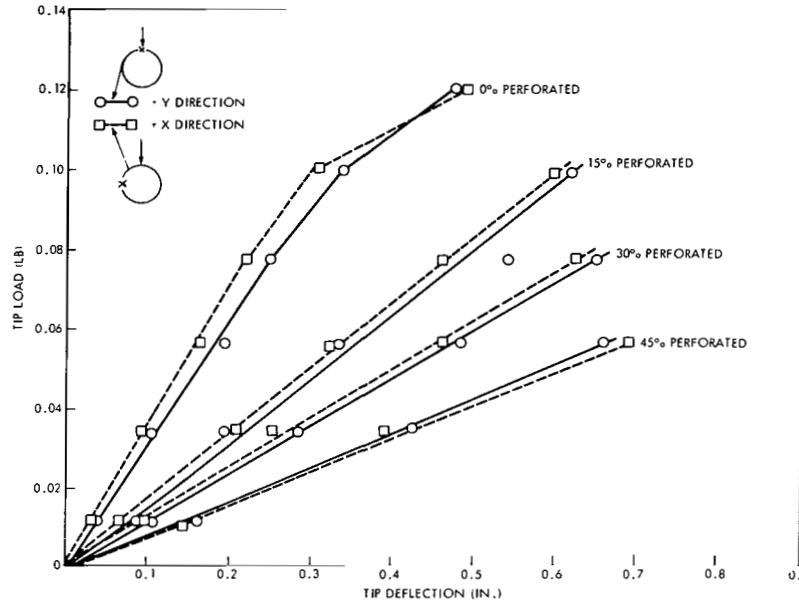

Figure 10–Load-deflection curve of a perforated interlocked Westinghouse cantilever clamped-free boom. Length, 32 in.; surface condition, BeCu alloy.

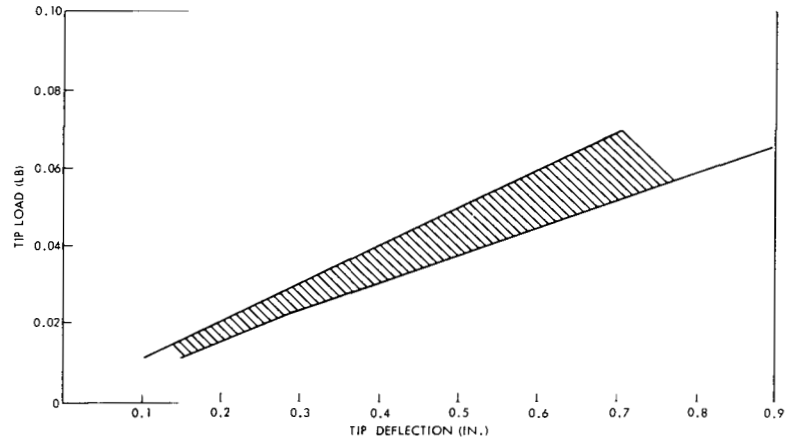

Figure 11–Load-deflection envelope representing all orientations and seam interlocking forces investigated for the 15% perforated interlocked Westinghouse booms. Length, 34.5 in.; surface condition, BeCu alloy.

closed boom exhibits a similar double-wall thickness as a result of interlocking tabs, but at the same time, due to the boom's ellipticity, the radius in the seam plane (y-plane) becomes measurably smaller. This in turn results in an overall reduction in the value of I for the y-plane to a value below that for the x-plane with a corresponding change reflected in EI levels. The effect of applied moment and seam tightness was investigated by dynamic means previously described; that is, boom elements 35 in. long were subjected to initial tip displacements of 0.25 in. and 1.0 in., which represent substantial

differences in the degree of root stressing. These data show that for small tip deflections, the maximum effect of seam tightness on EI was less then 8% for either plane of loading and less than 5% for the larger deflection case. On the other hand, for a given degree of tightness and depending upon the magnitude of tip loading, EI was altered markedly. Specifically, EI determinations for both tight and moderately tight seams appear to be about 15% to 20% higher for the low bending moment condition than for the higher loading case. The same trend is evident in the loose seam boom but only to the extent of approximately 9%. The reduction in EI as a function of increased bending moment is explained by the inevitable factor of increased air damping along with nonlinearity associated with cross-sectional deformation behavior of the booms at the higher loading condition. The fact that static EI values were consistently lower than dynamic EI values is also attributed to the influence of the nonlinear relationship between tip load versus tip deflection curves at the higher bending load. In line with previous EI behavior determined statically, the dynamic EI value in the x-plane was greater than the value determined in the y-plane. Specifically, for the low and high bending moments, the corresponding increase in EI was measured to be about 14% and 17%, respectively.

Vibration Frequency

During dynamic testing it was observed that the boom tip traced out a complex oscillatory pattern as its amplitude of transverse bending decayed. This compound motion, illustrated in Figure 12, was detected by photographically monitoring a light source mounted on the tip of a 43-ft-long boom after initial displacement and release.

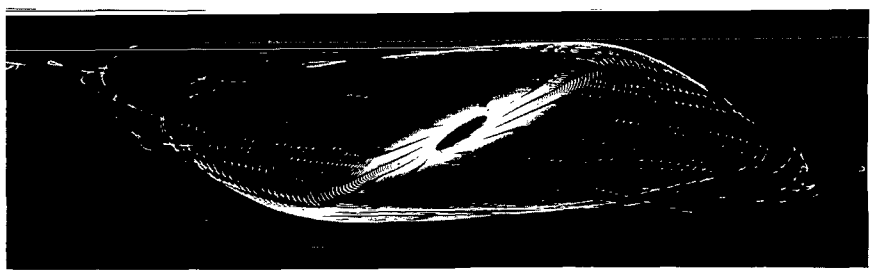

To measure the transverse vibration frequencies of shorter booms, each element in the x- and y-planes was excited separately and the corresponding oscillations were recorded. The resulting transverse bending frequencies are presented in Table 3.

When the booms were initially set into vibration in a plane other than a plane of symmetry, the decaying vibration plane was observed to precess about the boom axis in an oscillatory manner, very similar to the behavior noted in the Mink paper, and registers as a "beating characteristic," a typical example of which is shown in Figure 13. This behavior is ascribed primarily to significant boom EI variations due to nonsymmetrical section properties along with a small contribution of twisting that is dynamically coupled with the transverse bending mode.

Table 3-Transverse bending vibration frequency (Hz).

Boom design	Length (in.)	Frequency (Hz)		Frequency Difference $F_y - F_x$(Hz)	Measured Beat Frequency (Hz)
		x-plane	y-plane		
BeCu overlapped SPAR-STEM straight seam	34.1	11.4	14.1	2.7	2.5
Molybdenum overlapped					
Straight seam	35.0	13.0	16.0	3.0	3.0
Twisted seam (45°/36 in.)	35.0	14.0	15.0	1.0	1.0
Wire grid overlapped					
12 x 17 mesh	35.0	10.5	12.5	2.0	2.0
12 x 12 mesh	35.0	14.0	15.0	1.0	1.0
BeCu interlocked					
0% perforations	34.5	12.5	12.2	0.30	0.24
15% perforations	34.5	11.1	10.1	1.00	0.96
30% perforations	34.6	9.9	9.2	0.70	0.71
45% perforations	34.7	9.3	8.5	0.80	0.70
15% perforations, tight seam	35.0	10.7	10.0	0.70	0.70
15% perforations, moderately tight seam	35.0	10.5	9.8	0.70	0.72
15% perforations, loose seam	35.0	10.4	9.7	0.70	0.72

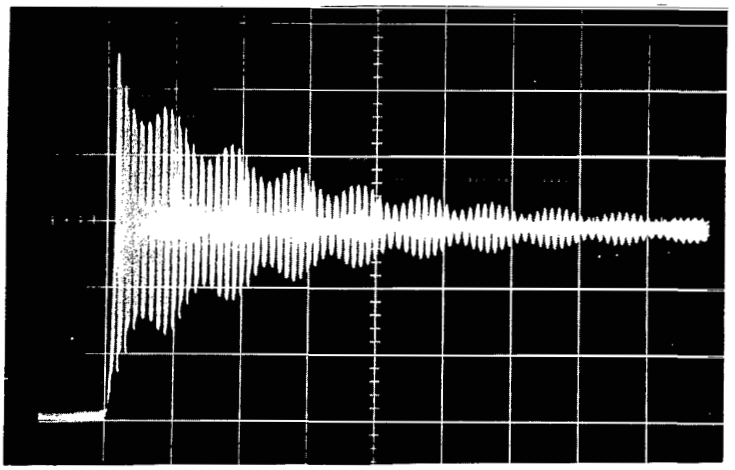

Figure 13–Decaying vibration amplitude of a Westinghouse tube measured in the x-direction, plucked in a direction between the x- and y-planes. Note the lower torsional vibration frequency modulating the natural x-plane bending frequency.

The magnitude of this "beat" frequency is a function of boom configuration and is equivalent to the difference in transverse bending frequencies corresponding to the x- and y-planes. These beat frequencies, which are presented in Table 3, must not be construed as necessarily being related to the natural frequency of the boom in torsional vibration, despite the fact that the boom experiences dynamic coupling (bending plus twist) when excited in a plane other than the plane of symmetry. The overlapped booms exhibited higher bending frequencies in the seam plane than the interlocked boom. The bending frequencies of the overlapped booms were generally higher than those measured on the interlocked boom.

Critical Bending Moment

Very-thin-walled cylinders fail in bending from localized buckling at loads substantially below the yield strength of the material. This failure mode has been confirmed experimentally* on tests of overlapped SPAR-STEM structures. Critical bending moment was determined with the test setup shown in Figure 2, tip loading of a horizontally clamped-free boom. Similarly, the loads were applied incrementally to the point at which the tubular structure failed suddenly in compression. The consequent buckling moment is then simply the product of boom length and failure load including the contribution from tare weight. In the case of the Westinghouse boom samples, it was possible to determine this critical parameter by two additional methods with equipment furnished by the manufacturer. The equipment was, specifically, a spacecraft deployer to simulate end-fixity conditions expected in service and a test apparatus (Figure 14) designed to impart uniform loading over the entire test section. With the deployment mechanism, structural instability (collapse) was induced by applying a 1-lb tip mass and then extending the boom horizontally to failure. Using the pure bending device offers several advantages besides permitting the application of a constant bending moment. Sample size is relatively unimportant in determining critical bending moment.

In addition, any flaw or surface defect along the entire test section is subjected to the same bending moment, which promotes failure at the weakened site. This particular testing apparatus is capable of applying a constant moment of up to 24 in.-lb for specimen lengths of 3 ft or longer. As shown in Figure 12, the bending moment was increased by varying the magnitude of opposing forces applied horizontally 3 in. apart using calibrated weights. The results of these tests are summarized in Table 4 for the various booms investigated.

Overlapped BeCu Alloy SPAR-STEM

In the course of testing the overlapped SPAR-STEM, the direction and plane of minimum bending was determined by observation of the onset of seam warping as the tip was loaded consecutively in the $+x$, $-x$, $+y$, and $-y$ orientations. As indicated in Table 4, the minimum critical buckling moment turned out to be 7.2 in.-lb with the

*Grimsley, J.D., and Phenix, J. E., Materials R&D Branch, Report to W. Scull, OGO Project Officer. GSFC memo, March 19, 1968.

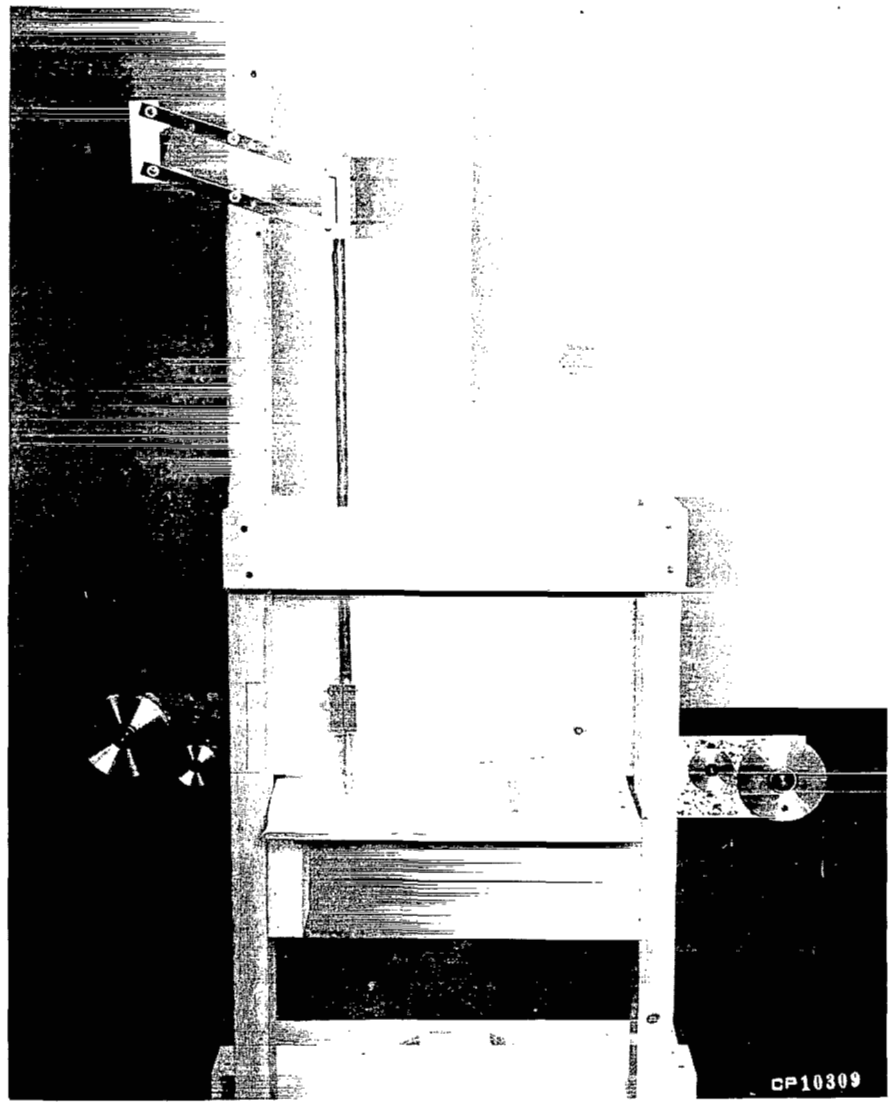

Figure 14–Bending tester.

origin of failure approximately 18 in. from the root of the 36-in.-long test sections. As the test proceeded, excessive warping (edge deformation) was observed to occur at the overlapped seam. This represents a localized elastic instability condition arising because no shear can be transmitted across the overlapped region except possibly by coulomb friction forces between contacting surfaces. With increasing load, the buckling strength of the boom is exceeded and failure occurs in the region where the deformation is most severe.

In the course of conducting cyclic load tests, which will be discussed in a later section, samples of identical length (8.5 in.) were also used to determine the critical bending moment of the SPAR-STEM and the Westinghouse boom. The critical bending moments of the 8.5-in.-long overlapped specimens were 34 in.-lb in the $+y$-direction (direction

Table 4-Critical bending moment.

Boom design	Length (in.)	Direction and plane of bending	Critical bending moment (in.-lb)	End-fixity conditions
BeCu overlapped SPAR-STEM	8.5*	$-x$	16.0	Clamped-free cantilever
	8.5*	$+y$	34.2	Clamped-free cantilever
	36.0	$+x$	7.2	Clamped-free cantilever
Molybdenum overlapped, straight seam	35.0	$-x$	6.6	Clamped-free cantilever
	35.0	$+x$	5.8	Clamped-free cantilever
Wire grid overlapped, 12 X 17 mesh	35.0	$+x$	10.5	Clamped-free cantilever
	31.5	$-x$	10.2	Clamped-free cantilever
BeCu interlocked, 15% perforations	8.5*	$-x$	6.0	Clamped-free cantilever
	8.5*	$+y$	8.2	Clamped-free cantilever
	8.5*	$+x$	8.5	Clamped-free cantilever
	24.0	$+y$	8.5	Clamped-free cantilever
	40.8	$+x$	8.7	Clamped-free cantilever
	31.5	$-x$	8.2	Clamped-free cantilever
	31.5	$-y$	6.4	Clamped-free cantilever
	40.8	$+y$	7.8	Clamped-free cantilever
	12.0	$+y$	8.8	Deployer clamped cantilever
	12.0	$+x$	5.8	Deployer clamped cantilever
	12.0	$-y$	7.5	Deployer clamped cantilever
	28.4	$-y$	5.8	Four point bending

*Cyclic loading tests.

of the seam) and 16 in.-lb in the $-x$-direction. This marked difference in buckling behavior is largely attributed to variations in EI properties resulting from geometric changes in the SPAR-STEM's cross section that significantly reduce the value of I in the plane normal to the seam ($-x$-plane) and, consequently, its critical bending moment. The increase in bending moment observed for the shorter boom (16.0 in.-lb) in contrast to the longer section (7.2 in.-lb) for the same plane of loading (the x-plane) is primarily the result of end constraints imposed on each boom. For the short boom, the tip and root are essentially rigidly clamped, which prevents seam warping and thereby increases buckling strength. However, with increasing length, load application through the shear center of the overlapped section becomes progressively more difficult, resulting inevitably in substantial twisting, which in turn degrades boom strength.

Overlapped Molybdenum Thin-Walled Tube

Critical bending moments attained by the molybdenum tube for a given tip loading direction in the x-plane show a small but significant difference in magnitude. As indicated in Table 4, critical buckling strengths were 5.8 in.-lb in the $+x$-direction and 6.6 in.-lb in the $-x$-direction for a 35-in.-long boom section. When the bending moment reached a level of 3.5 in.-lb, warping of the overlapped seam was observed to occur at a point 5 in. from the root as well as 6 in. from the tip. Simultaneously, the seam at the tip twisted approximately 90° relative to the root of the boom. At a bending moment of 4.3 in.-lb, the seam was observed to twist 180° with buckling occurring at a point 20 in. from the root with the application of a bending moment of 6.6 in.-lb. Similar behavior was observed with load applied in the $+x$-direction. Initial seam warping developed when the bending moment reached 4.7 in.-lb at 5.0 in. from the root and the tip twisted about 90° with respect to the root. Buckling occurred when the bending moment reached a value of 5.8 in.-lb with failure originating at a section 3 in. from the root.

Overlapped Wire Grid Thin-Walled Tube

As in the case of the two preceding overlapped designs, the minimum critical buckling strengths of the wire screen boom coincided with tip loading in the x-plane. In addition, the seam response to bending moment was similar to that exhibited by both the molybdenum and BeCu SPAR-STEM configurations. Specifically, as the bending moment reached a value of 5.9 in.-lb, the seam at the tip correspondingly twisted about 45° relative to the root of the test boom.

As the bending moment increased to 8.2 in.-lb, the seam opened up at a point 2.5 in. from the tip of the boom. Separation of the seam edges continued with increasing bending moment until, at 9.7 in.-lb, the resulting gap in the vicinity of the tip approached 135°. During the period of loading, the seam rotated about 90° with respect to its initial root position. At a critical bending moment of 10.5 in.-lb, the boom failed by local buckling near the root section.

In the case of the 31.5-in.-long boom tip loaded in the $-x$-plane, the seam twisted about 25° at a bending moment of 4.6 in.-lb. Subsequently, at a bending moment of 5.3 in.-lb, the seam opened up about 11 in. from the tip. When the boom was subjected to 9.5 in.-lb bending moment, the seam twisted 90° about the boom axes and opened up both at the clamp and the tip. Finally, buckling occurred at a maximum bending moment of 10.2 in.-lb, approximately 7 in. from the clamped end.

Interlocked Perforated Westinghouse Booms

As indicated earlier, three test methods were employed to evaluate the Westinghouse boom: a clamped-free cantilever, a deployer clamped-free cantilever, and a device for applying a constant bending moment. Critical buckling strengths corresponding to each test method are presented in Table 4. Within experimental error and taking sample variation into account, buckling strength appears insensitive to sample length, plane of loading, and method of testing. This uniformity in critical bending moment of the interlocked boom is attributed to the fact that its section properties more nearly matched those of an ideal thin-walled cylinder. In contrast, the value of I for the three open cross-sectional booms can vary markedly with seam orientations and degree of overlap. In all cases, however, compression buckling invariably was the dominant failure mode. For the clamped-free condition, critical buckling always originated near the root support where bending moment (and stress) is at a maximum. On the average, the interlocked samples exhibited a mean buckling strength of 7.5 in.-lb associated with a 14.5% variation.

Damping

Damping behavior of gravity gradient booms and antennae are important to spacecraft design for the prediction of service performance. A measure of this dynamic property is given as logarithmic decrement δ, which is obtained from the slope of vibration amplitude versus cycles curves plotted on semilog paper.

Previously, vibration decay rates of 43-ft-long deployer clamped SPAR-STEM's (Reference 7) under vacuum conditions were determined by means of both strain gage and photographic techniques. It was concluded from these results that the magnitude of damping for the overlapped configurations (bare and electroplated) was small and that coulomb friction generated between overlapping surfaces constituted the principal mechanism for dissipating energy. In addition, photographic and strain gage data showed good agreement in describing the dynamic response of the SPAR-STEM design. A typical example of boom tip motion recorded by photographic time exposures is illustrated in Figure 12.

After the establishment of this advanced boom study, additional damping data*, all of which are presented in Table 5, were generated and compared with the dynamic

*Hershfeld, D. J., "RAE Boom Damping Study in the Dynamics Test Chamber." GSFC memo, August 17, 1965.

Table 5-Boom damping properties.

Boom design	Length	Test pressure (torr)	Bending moment	Logarithmic decrement δ							Average	Surface condition
				x-plane			y-plane			x, y-plane		
				Strain gage	Photo-graphic	Optical tracker	Strain gage	Photo-graphic	Optical tracker	Photo-graphic		
BeCu overlapped SPAR-STEM	43 ft	2×10^{-2}		0.0085	0.0081							Ag plated
	43 ft	2×10^{-2}		.0240	.0276							Unplated
	43 ft	2×10^{-2}		.0070	.0074		0.0045	0.0066			0.019	Ag and Cd plated
	43 ft	2×10^{-2}		.0085	.0083		.0136	.0267				Ag and Cd plated
	28 ft	2×10^{-2}		.0230	.0470		.0410	.0470				Ag and Cd plated
	10 ft	2×10^{-2}								0.066		Unplated
	10 ft	2×10^{-2}								.051	.059	Ag plated
	10 ft	2×10^{-2}								.061		Ag and Cd plated
Molybdenum overlapped												
Straight seam	35.0 in.	760	1.3			0.103			0.077		.074	Unplated
Twisted	35.0 in.	760	1.4			.049			.067			Unplated
Wire grid overlapped												
12 × 17 mesh	35.0 in.	760	4.4			.184			.072		.164	Elgiloy, longitudinal wire
12 × 12 mesh	35.0 in.	760	4.0			.316			.083			BeCu, transverse wire
12 × 17 mesh	35.0 in.	760	1.1			.051			.058		.054	
BeCu interlocked												
0% perforations	10 ft	2×10^{-2}								.014		Al plated
15% perforations	10 ft	2×10^{-2}								.012	.014	Al plated
45% perforations	10 ft	2×10^{-2}								.017		Al plated
0% perforations	34.5 in.	760	2.4			.012			.044			Unplated
15% perforations	34.5 in.	760	1.3			.031			.031		.034	Unplated
30% perforations	34.6 in.	760	.9			.039			.039			Unplated
45% perforations	34.7 in.	760	.6			.035			.044			Unplated
15% perforations, tight seam	35.0 in.	760	.6			.014			.021			Unplated
15% perforations, moderately tight seam	35.0 in.	760	.6			.015			.021		.018	Unplated
15% perforations, loose seam	35.0 in.	760	.6			.019			.019			Unplated
15% perforations, tight seam	35.0 in.	760	2.5			.038			.058			Unplated
15% perforations, moderately tight seam	35.0 in.	760	2.5			.046			.074		.047	Unplated
15% perforations, loose seam	35.0 in.	760	2.5			.028			.038			Unplated

behavior of the SPAR-STEM. As a point of information, variation in sample length of the previously mentioned damping experiments was accomplished with a commandable deployment mechanism.

As noted in Table 5, booms less than 3 ft in length were tested in air, and the 10-ft samples were evaluated in a vacuum environment of approximately 2×10^{-2} torr. The short booms were clamped vertically at their base with the free end up, and the 10-ft samples were vertically clamped with the free end suspended down to avoid buckling the element. The amplitude decay and frequency of the short booms were measured with the optical tracker described earlier. The vibration decay of the boom tip in the z-plane was experimentally determined for the 10-ft-long samples by strain gage instrumentation at the root of the supporting mandrel and by photographic recordings of the boom tip motion.

Damping constants of the mandrel clamped 10-ft-long SPAR-STEM's were significantly higher than similarly tested interlocked booms of equal length. Previous analysis has demonstrated that damping of BeCu boom structures consists essentially of internal friction and coulomb damping. At low stresses, internal friction of BeCu is extremely small (e.g., $\delta = 5 \times 10^{-4}$) and thus considered to be negligible. Coulomb friction, generated by the cyclic sliding (shear displacement) action of seam surfaces in contact, is at least an order of magnitude greater and, therefore, constitutes the primary damping mechanism.

It has been demonstrated* that boom damping is markedly influenced by end-fixity conditions and sample length; thus it is not surprising to note that for the SPAR-STEM, the 10-ft-long boom exhibits markedly higher damping than the previously tested 28-ft- and 43-ft-long SPAR-STEM's that were deployer clamped rather than mandrel supported. Since bending stresses and high frequency vibrations are concentrated within approximately the first 15 ft from the boom root, it follows that in this region most of the energy is dissipated. Thus, for a given applied bending moment, the magnitude of total energy developed per cycle increases with length, but since friction damping dissipates equal amounts of energy per cycle, it is evident that shorter booms will be damped out more rapidly.

The method of determining damping behavior of the short (3-ft-long) booms tested in air corresponds essentially to the techniques used in evaluating the longer booms. That is, the vertically supported boom is displaced laterally a given amount and released in a direction that excites only the bending vibration mode in either the x- or y-plane. Damping decrements are subsequently established from the resulting vibration decay curves. In these experiments with short booms, however, viscous air damping contributes also to total damping performance, along with internal friction and coulomb damping. The results of Table 5, however, indicate that the magnitude of this effect is relatively small. Specifically, average damping decrements for the 3-ft- and 10-ft-long interlocked booms are $\delta = 0.018$ and $\delta = 0.014$, respectively, and thus constitute reasonable measures

*Phenix, J. E., "Damping of Kapton Coated BeCu Booms." GSFC memo, February 12, 1968.

of self-damping behavior. For short booms representing various degrees of seam tightness, a significant increase in damping is observed when the applied bending moment is increased from 0.6 in.-lb to 2.5 in.-lb corresponding to decrements of $\delta = 0.018$ and $\delta = 0.047$, respectively. Varying the degree of open hole area (% perforations) does not appear to change the damping decrement nearly as much as changing the level of applied moment. This is illustrated by the data obtained on the 10-ft-long booms. The observed increase in the damping constant with an increase in bending moment results from the increase in coulomb (sliding friction) damping at the seam and the added contributions of internal friction with magnitude of stress.

The molybdenum booms exhibited an average damping constant of $\delta = 0.074$, in reasonable agreement with 10-ft-long SPAR-STEM results for small (≈ 1 in.-lb) bending moment. Since both thin-walled configurations are identical and internal friction of molybdenum is essentially the same as that for BeCu, the damping similarity was not unexpected.

Approximately the same level of coulomb damping ($\delta = 0.054$) was also observed for the overlapped wire grid boom design subjected to small initial bending moment. However, for relatively large maximum applied bending moment (≈ 4 in.-lb), damping was not only substantially increased but was sharply influenced by the initial plane of loading. In the y-direction (seam plane) the measured average damping decrement δ was 0.071, but in the x-direction, energy dissipation was so pronounced that the average log decrement δ increased to 0.250. It was interesting to note that regardless of the direction initially selected for boom displacement, the ultimate vibration mode shifted invariably to the y-plane. This phenomenon of damping attenuation is related to the extremely high interference friction developed as a consequence of the exposed edge wires in the overlapping seam intersecting the wire mesh.

Critical Bending Moment Under Cyclic Loading

It is possible for booms in service to develop oscillatory motion from a variety of factors such as thermal excitation (e.g., OGO-4), orbit eccentricity (e.g., ATS-2), and even from the pulsing action of attitude control systems. Whatever the driving force may be, the ultimate result is some complex form of cyclic bending that could induce root fiber stresses above the material's endurance limit and cause eventual failure.

In view of this possible potential failure mode, a limited investigation of boom samples representing the SPAR-STEM and Westinghouse configurations was conducted under stress conditions far exceeding service requirements. Specifically, the maximum bending moment anticipated for a 1000-ft-long boom vibrating with a tip amplitude of 500 ft was assumed. An estimate of maximum bending moment is obtained by Equation 3:

$$M = \frac{3YEI}{L^2}, \tag{3}$$

where

M = maximum bending moment (in.-lb)

Y = tip deflection (in.)

E = Young's modulus (19×10^6 psi)

I = moment of inertia (in.^{4})

L = boom length (in.).

The moment of inertia of the SPAR-STEM was assumed to be that for a tube, while the moment of inertia of the perforated Westinghouse boom was determined by Equation 4:

$$I = \pi \frac{r^3 t\,(S - D)}{S}, \tag{4}$$

where

S = window spacing (in.)

D = window diameter (in.)

r = boom radius (in.)

t = wall thickness (in.).

The maximum bending developed at the root was calculated to be 0.125 in.-lb. Bending moments of 2 in.-lb and 4 in.-lb, which increased the minimum loading severity more than 15 times that of the prescribed conditions, were selected for the test.

A cantilever boom 100 ft long exhibits a period of approximately 5 minutes when oscillating at its fundamental frequency; thus, if maximum deflections continued for a year, the boom would ultimately experience about 100 000 complete cycles. For this reason, cyclic loading of test samples was continued for at least 100 000 cycles of operations at the applied bending moments described above.

The test apparatus used to evaluate the boom samples is shown in Figure 15. The boom root was clamped onto a 0.5-in.-diameter mandrel, which in turn was affixed to the vise of a constant deflection fatigue machine. The boom tip was similarly clamped and then bolted securely to the crank of the eccentric. The boom sample was oriented with the seam on top and the eccentric set at zero. The tare weight of the end fixture was counterbalanced by a spring scale, and the initial position of the boom was recorded

at a point 8 in. from the root using a cathetometer. The counterbalance was then removed, and the eccentric set to provide the deflection necessary to impart the designated loads. Static stiffness and critical bending moment were measured for the boom segments with the same end fixtures as employed in the cycling test. During and after each test run, the surface of the boom was visually observed with a low power microscope for evidence of incipient cracking. The results are summarized in Table 6. The only evidence of damage attributed solely to the cycling action was an abraded area near the interlocking tabs (notches) of the Westinghouse boom. This galling condition at the root of the notches is explained by the inevitable axial rubbing action of adjacent tabs in mating contact. The boom eventually failed when the magnitude of bending moment exceeded the critical value of 9.5 in.-lb. It must be mentioned that the boom sample incurred a small buckle in the test region while inserting it in the test fixture. Consequently, it was not surprising to note that failure eventually occurred precisely at this weakened section. As indicated in Table 6, the Westinghouse boom was run at progressively higher bending loads until buckling failure occurred at 9.5 in.-lb after 5700 cycles. No evidence of fatigue damage was observed on the SPAR-STEM after similar testing at 2 in.-lb and 4 in.-lb levels with the same load-cycle procedure.

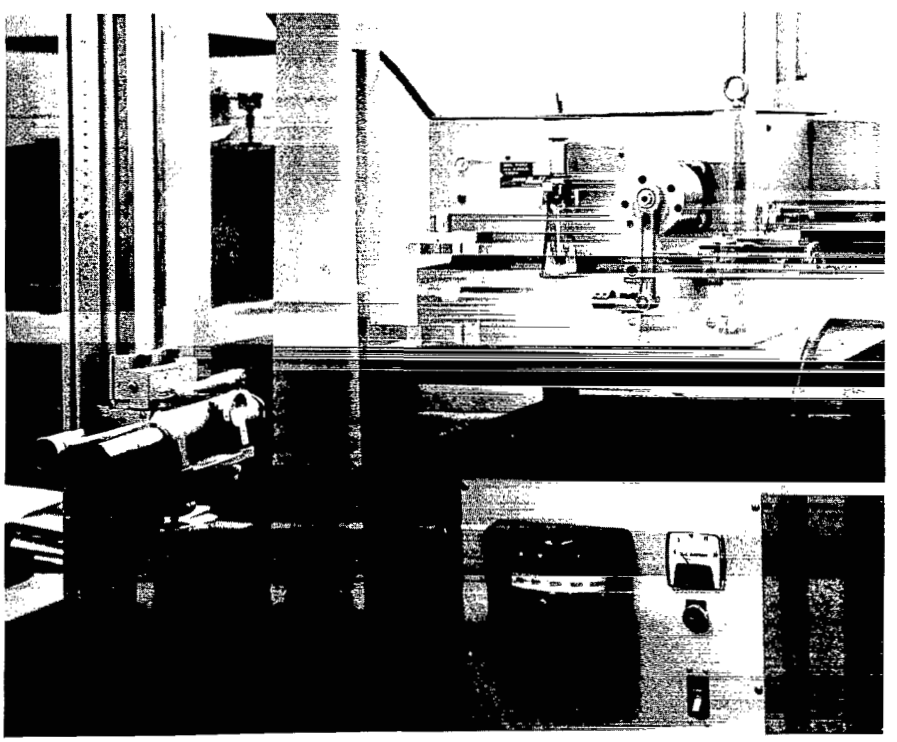

Figure 15–Apparatus for cyclic loading of boom segments.

Table 6-Fatigue test data on the Westinghouse and SPAR-STEM type of boom segments.

Boom	Maximum bending moment (in.-lb)	Maximum bending stress (psi)	Freq. (Hz)	Total cycles	Remarks
15% perforations, Westinghouse, 8.5 in.	2	9 500	475	561 300	
	4	19 000	460	111 900	
	9.5	46 000	430	5 700	Buckle prior to test/fatigue fracture at buckled area
SPAR-STEM, 8.5 in.	2	5 100	840	104 500	
	4	10 200	900	105 200	

Fatigue testing of heat-treated BeCu 190 alloy indicated the endurance limit to be approximately 55 000 psi. The bending stress expected in space flight as well as the stress levels achieved in this arbitrary test for 2 in.-lb and 4 in.-lb bending moments were well below this limit. Consequently, it was clearly demonstrated that vibration bending loads 30 times those anticipated in service would not produce cyclic failure of either the interlocked Westinghouse boom or SPAR-STEM.

SUMMARY AND CONCLUSIONS

The results of this investigation, which has evaluated several advanced boom configurations in terms of specific structural properties, are summarized in the following paragraphs.

Bending stiffness (EI) varied markedly with boom configuration, seam orientation, and test method. The overlapped booms exhibited higher EI about the axis normal to the x-section of the axis of symmetry in contrast to the interlocked boom, which was slightly stiffer about the axis of symmetry. This anomaly is related to the elliptical geometry of the zippered boom and the measurably smaller area moment of inertia developed in the plane of the seam. In general, the static EI values tended to be lower in magnitude than corresponding dynamic stiffness measurements. This is explained by the development of significantly higher root stressing and consequent nonlinear tip load tip deflection behavior promoted by clamped-free cantilevered booms.

Except for the 0% interlocked perforated condition, the overlapped booms invariably exhibited higher EI than the interlocked structure, regardless of seam orientation. In addition, x-plane stiffness of the interlocked booms was observed to be 10% to 20% greater than for y-plane loading, which is contrary to the bending behavior exhibited by the three overlapped booms. The theory for cylinders of open section appears to predict dynamic EI reasonably well, but is at least 20% higher than values obtained statically.

The interlocked boom exhibited structural buckling characteristics similar to the classical shell failures predicted for thin-walled seamless tubing under clamped-free end constraints. Furthermore, its critical buckling strength was apparently insensitive to sample length, plane of loading, and test method.

In marked contrast, the open (overlapped) thin-walled boom behaved in a complex manner peculiar to tubular structures whose cross-sectional properties vary in a non-symmetrical manner with increasing applied bending moment. In addition, sample length, together with end constraint conditions, plays a major role in buckling strength performance. Phenomenologically, buckling originates in the vicinity of the root region and manifests itself as a sequential failure mode that involves elastic edge kinking and complete separation and opening of the seam and finally results in sudden inelastic buckling.

It was clearly demonstrated that cyclic loading of short booms did not promote failure by an incipient (fatigue) cracking mechanism but rather by localized buckling when the critical bending moment was applied to the structure. At bending loads approximately 16 times greater than anticipated under service conditions, both the interlocked and SPAR-STEM configurations sustained more than twice the number of cycles each would experience if oscillated at their fundamental frequencies for a period of 1 year.

Coulomb damping (sliding friction of the seam) constitutes the principal mechanism of energy dissipation in boom structures. Damping, as described by logarithmic decrement, is influenced by end fixity, sample length, and level of bending load. Damping behavior of the three overlapped booms in lengths not exceeding 10 ft were approximately the same but were appreciably higher than the interlocked boom for bending moments nominally 1.0 in.-lb. At relatively high bending loads (~ 4.0 in.-lb), damping of the wire mesh element appeared to be seam orientation dependent, with significantly higher values in the plane normal to the seam. For the interlocked boom, damping was markedly affected by the magnitude of applied bending moment rather than by the percentage of surface area perforated.

Clamped-free booms trace out a complex vibration pattern that follows a revolving ellipsoidal path and is attributed principally to variations in cross-sectional properties (specifically stiffness) when excited in a plane other than the plane of symmetry.

ACKNOWLEDGMENTS

The authors wish to gratefully acknowledge the technical support provided by Miss Jane Jellison, Mr. James Jarrett, and Mr. Henry Sweet of the Materials Research and Development Branch for their efforts in setting up the instrumentation, boom preparation, and recording of test data.

Goddard Space Flight Center
National Aeronautics and Space Administration
Greenbelt, Maryland, February 5, 1970
604-31-75-01-51

REFERENCES

1. Rimrott, F.P.J., "Storable Tubular Extendable—A Unique Machine Element," Machine Design 37(29): 155-165, December 1965.

2. "Gravity Gradient System for Antenna Structures," NASA RFP PC #620-3394, November 1964.

3. "Development of Molybdenum Gravity Gradient Rods," General Electric Document No. 68SD4256, NAS5-10323, May 8, 1968.

4. "Gravity Gradient Boom and Antenna Material Study," General Dynamics/Convair Division GDC-ZZ67-010, NAS5-9597, August 18, 1967.

5. "The Refinement of Gravity Gradient Booms and Deployers," General Dynamics/ Convair Division GDC-ZZL68-001, NAS5-10376, February 1, 1968.

6. Frisch, Harold P., "Thermal Bending Plus Twist of a Thin-Walled Cylinder of Open Section With Application to Gravity Gradient Booms," NASA Technical Note D-4069, August 1967.

7. Predmore, R. E., Staugaitis, C. L., and Jellison, J. E., "Damping Behavior of DeHavilland STEM Booms," NASA Technical Note D-3996, June 1967.

02U 001 56 51 3DS 70254 0090
AIR FORCE WEAPONS LABORATORY /WLOL/
KIRTLAND AFB, NEW MEXICO 87117

ATT E. LOU BOWMAN, CHIEF,TECH. LIBRAR

"The aeronautical and space activities of the United States shall be conducted so as to contribute . . . to the expansion of human knowledge of phenomena in the atmosphere and space. The Administration shall provide for the widest practicable and appropriate dissemination of information concerning its activities and the results thereof."

—NATIONAL AERONAUTICS AND SPACE ACT OF 1958

NASA SCIENTIFIC AND TECHNICAL PUBLICATIONS

TECHNICAL REPORTS: Scientific and technical information considered important, complete, and a lasting contribution to existing knowledge.

TECHNICAL NOTES: Information less broad in scope but nevertheless of importance as a contribution to existing knowledge.

TECHNICAL MEMORANDUMS: Information receiving limited distribution because of preliminary data, security classification, or other reasons.

CONTRACTOR REPORTS: Scientific and technical information generated under a NASA contract or grant and considered an important contribution to existing knowledge.

TECHNICAL TRANSLATIONS: Information published in a foreign language considered to merit NASA distribution in English.

SPECIAL PUBLICATIONS: Information derived from or of value to NASA activities. Publications include conference proceedings, monographs, data compilations, handbooks, sourcebooks, and special bibliographies.

TECHNOLOGY UTILIZATION PUBLICATIONS: Information on technology used by NASA that may be of particular interest in commercial and other non-aerospace applications. Publications include Tech Briefs, Technology Utilization Reports and Notes, and Technology Surveys.

Details on the availability of these publications may be obtained from:

SCIENTIFIC AND TECHNICAL INFORMATION DIVISION

NATIONAL AERONAUTICS AND SPACE ADMINISTRATION

Washington, D.C. 20546